Modeling the Reduction of Hydrogen Peroxide by Glutathione Peroxidase Mimics

ARTICLE *in* THE JOURNAL OF PHYSICAL CHEMISTRY A · AUGUST 2006

Impact Factor: 2.69 · DOI: 10.1021/jp0615196 · Source: PubMed

2 AUTHORS:

Jason K Pearson
University of Prince Edward Island
28 PUBLICATIONS **240** CITATIONS
SEE PROFILE

Russell J Boyd
Dalhousie University
304 PUBLICATIONS **6,030** CITATIONS
SEE PROFILE

Modeling the Reduction of Hydrogen Peroxide by Glutathione Peroxidase Mimics

Jason K. Pearson and Russell J. Boyd*

Department of Chemistry, Dalhousie University, Halifax, Nova Scotia B3H 4J3, Canada

Received: March 12, 2006; In Final Form: May 5, 2006

Theoretical calculations have been performed on three model reactions representing the reduction of hydrogen peroxide by ebselen, ebselen selenol, and ebselen diselenide. The reaction surfaces have been investigated at the B3PW91/6-311G(2df,p) level, and single-point energies were calculated using the 6-311++G(3df,3pd) basis set. Solvent effects were included implicitly with the conductor-like polarizable continuum model and in one case with explicit inclusion of three water molecules. Mechanistic information is gained from investigating the critical points using the quantum theory of atoms in molecules. The barriers for the reduction of hydrogen peroxide with the ebselen, ebselen selenol, and ebselen diselenide models are 56.7, 53.4, and 35.3 kcal/mol, respectively, suggesting that ebselen diselenide may be the most active antioxidant in the ebselen GPx redox pathway. Results are also compared to that of the sulfur analogues of the model compounds.

Introduction

Selenium is essential to the reductive ability of several mammalian antioxidant enzymes, most notably the glutathione peroxidase (GPx) family.[1−5] GPx catalyzes the reduction of harmful peroxides by the thiol glutathione (GSH), and this process protects the lipid membranes and other cellular components against oxidative damage, which has been implicated in a variety of degenerative human conditions including various disease states and even the aging process.[6,7] Figure 1 illustrates the basic catalytic cycle of GPx.[8−10] The selenium moiety of the selenocysteine (Sec) residue of the enzyme (Enzyme-Se-H) is oxidized to the selenenic acid derivative (Enzyme-Se-OH) by reduction of a peroxide to the corresponding alcohol. GSH will then convert the selenenic acid to a selenenyl sulfide (Enzyme-Se-S-G) intermediate. To complete the cycle, a second GSH converts the sulfide intermediate back to the original selenol by liberating the oxidized glutathione (GSSG). Thus, two GSH molecules are consumed in the process, generating GSSG.

The intermediates and complexes of the catalytic cycle of GPx are chemically or kinetically unstable.[11] This makes it difficult to determine precise mechanistic details about their activity. As a consequence of such difficulty, the GPx family and other selenoproteins have ill-defined biological roles[11] despite a great deal of experimental investigation.[12] Theoretical modeling of this system or other selenoproteins has been relatively underutilized. Molecular mechanics methods have been used to model the full catalytic cycle,[11] and the redox chemistry of small molecule GPx mimics has been investigated with ab initio and DFT methods. [13]

There have been many attempts to mimic GPx activity with model systems[14−22] such as diselenides[14−16,19,20,23−25] and allyl selenides;[16] however, none have received more attention than ebselen (**1**) (2-phenyl-1,2-benzisoselenazol-3(2H)-one). Ebselen is a cyclic selenamide that has been extensively studied as an antioxidant and GPx mimic[26−31] and has recently been identified as a substrate for another selenoprotein, thioredoxin reductase (TrxR).[32] While there have been many proposed GPx mimics,

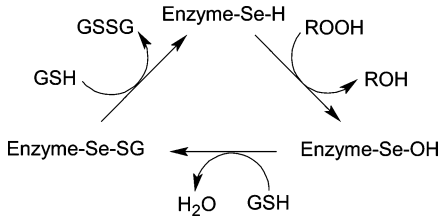

Figure 1. The catalytic cycle of GPx.

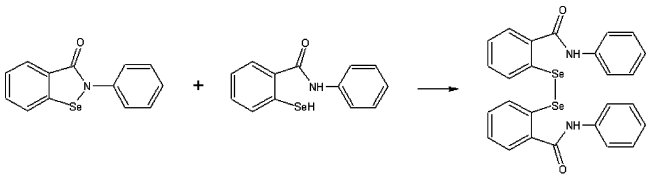

Figure 2. Reaction between ebselen (**1**) and ebselen selenol (**2**) to form ebselen diselenide (**3**).[45]

ebselen was the first compound to be used in clinical trials[33−35] and has attracted notable interest because of its anti-inflammatory, antiatherosclerotic, and cytoprotective properties in both in vitro and in vivo models.[36−41] These benefits are in part due to the fact that the selenium moiety in ebselen is not liberated during its biotransformation and thus cannot enter the selenium metabolism of the organism.[42−44]

The structure of ebselen does not closely resemble that of the active site Sec residue in GPx primarily because of the lack of a selenol moiety, although the selenol analogue of ebselen does exist. Ebselen has been shown to react with its selenol (**2**) to form a diselenide (**3**)[45] (see Figure 2). At this time, it is unclear which of these three molecules may be the most active form toward reduction of hydroperoxides. Several variations have been proposed,[45−50] yet there is still debate as to the exact mechanism by which ebselen functions as an antioxidant. A summary of proposed mechanisms is shown in Figure 3. While they all may contribute under the appropriate conditions, it would be advantageous to ascertain more precise information about the redox behavior of ebselen because the development of other, more active GPx mimics is a major objective for

* Corresponding author. E-mail: russell.boyd@dal.ca.

10.1021/jp0615196 CCC: $33.50
Published on Web 06/17/2006

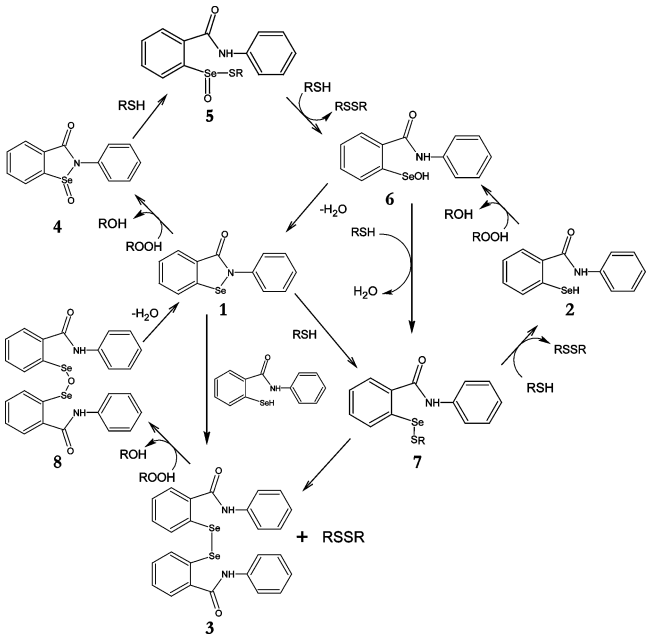

Figure 3. A summary of proposed catalytic schemes involving reduction of peroxides by ebselen (**1**), ebselen selenol (**2**), and ebselen diselenide (**3**).

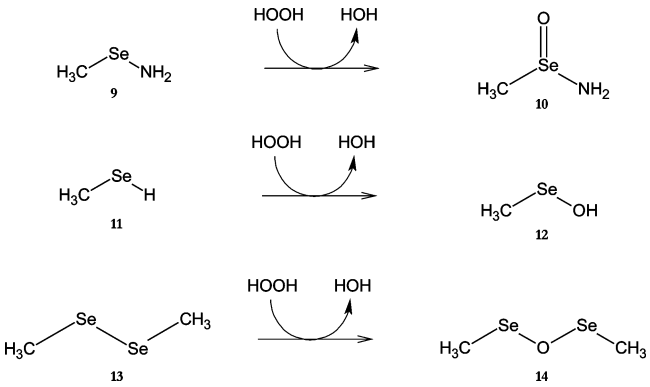

Figure 4. The three model reactions used in this study.

researchers to date. A proper understanding of the fundamental chemistry involved could bring with it the ability to predict successful candidates for better antioxidants.

To clarify the roles of each of these compounds and learn more about the reductive abilities of organoselenium compounds in general, the reduction of hydrogen peroxide by ebselen, ebselen selenol, and ebselen diselenide (see Figure 3) has been modeled with and without incorporating the effects of solvent using a computational scheme recently proposed for organoselenium compounds.[51] Because of the fact that sulfur analogues of selenoenzymes are considerably less effective in catalyzing reductive processes than their selenium-containing counterparts, a parallel study using the sulfur analogues was completed. Model compounds chosen to represent those in Figure 3 are shown in Figure 4. All processes involve the reduction of hydrogen peroxide to yield the oxidized organoselenium compound and water.

A possible explanation for the enhanced reductive ability of Se over S is the fact that Se has a lower pK_a, meaning that the Se−H bond in a selenol should be considerably weaker than the analogous S−H bond. As a consequence, the deprotonated Se anion may play a prominent role in organoselenium reduction of peroxides. To test this hypothesis, the reduction of hydrogen peroxide by the deprotonated ebselen selenol anion will be modeled and compared to that of the neutral molecule. The reaction profile will provide valuable information as to the likelihood of this alternative.

Computational Methods

Calculations for this paper were performed with the Gaussian 03[52] suite of programs. Geometry optimizations were performed with Becke's three-parameter exchange functional[53] (B3) in conjunction with the correlation functional proposed by Perdew and Wang[54] (PW91) using a 6-311G(2df,p) basis set as suggested recently for the reliable prediction of organoselenium geometries and energetics.[51] Transition states were located using Schlegel's synchronous transit-guided quasi-Newton (STQN) method[55,56] and were linked to reactant and product complex structures by the use of an intrinsic reaction coordinate calculation.[57,58] Frequency calculations were performed on all optimized structures using the B3PW91/6-311G(2df,p) method to obtain accurate thermochemical data and to confirm whether a structure is a minimum or first-order saddle point, etc. Accurate energies were obtained for all structures via single-point calculations using the 6-311++(3df,3pd) Pople basis set with the above DFT method. Solvent effects were incorporated implicitly with single-point calculations using the conductor-like polarizable continuum model (CPCM) at the B3PW91/6-311++G(3df,3pd) level and explicitly (for the case of the selenol anion reaction) with the inclusion of three water molecules. Also, for the case of the selenol anion reaction, diffuse functions were included on heavy atoms for the geometry optimizations and frequency calculations as well as in the transition state searches.

The topology of the electron density was examined with the AIM2000 software package[59,60] using the wave function obtained by the B3PW91/6-311G(2df,p) computational method.

Results and Discussion

Our results are illustrated in Figures 5−7. Part a of these figures illustrates the Gibbs free energies (in kcal/mol) of the reactant complex (RC), transition states (TS), and product complexes (PC), as well as the sum of the energies of the isolated products, all relative to the sum of the energies of the isolated reactants. Part b of these figures presents a pictorial view of the results from calculations using Bader's quantum theory of atoms in molecules (AIM).[61] AIM has been shown to provide valuable information about many different chemical systems by an analysis of molecular electron density distributions. Moreover, AIM is relatively insensitive to the theoretical method used to generate the wave function. In this context, the reaction species are examined to yield the details of the chemical bonding throughout the course of a particular reaction for the purpose of gaining mechanistic information. Part b of Figures 5−7 shows the positions of the maxima in the electron density (nuclei) and the bond paths connecting the nuclei, as well as the positions of the bond critical points (BCP), ring critical points (RCP), and in one case (RC in Figure 7b) a cage critical point (CCP). Interestingly, it is well known that finding a CCP inside a single ring is mathematically possible; however, it has remained illusive until very recently.[62] It should be noted that this is only the second example to date of a cage critical point found inside a single ring. Tables 1−3 accompany these figures as they present the relevant data for interpretation.

Ebselen Oxidation. Fischer and Dereu[47] were the first to investigate experimentally the reduction of hydrogen peroxide by ebselen in 1987. At that time, the precise mechanism was unknown; however, it was apparent that the reaction was fast and exothermic, resulting in the oxidized ebselen (**4**) molecule

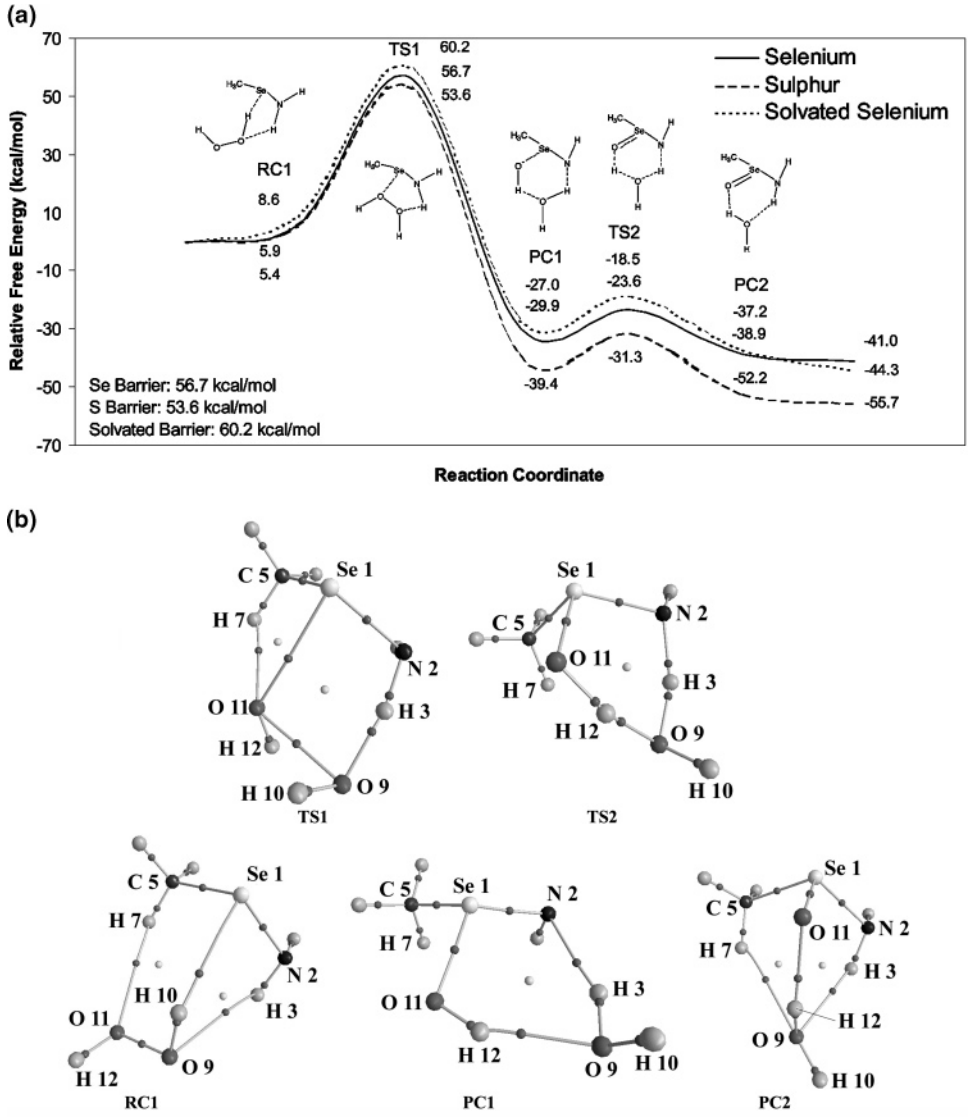

Figure 5. (a) Reaction energy profile for the model ebselen reaction with hydrogen peroxide. Results are also presented for the sulfur analogue of the ebselen model as well as the solvated selenium case. (b) Molecular graph of the first reactant complex (RC1), first transition state (TS1), first product complex (PC1), second transition state (TS2), and second product complex (PC2) showing positions of all nuclei, bond critical points (BCPs), and ring critical points (RCPs).

shown in Figure 3. It is noted that the oxidation of 2-benzyl-1,2-benzisoselenazol-3(2H)-one (ebselen with a methylene located between the N and the phenyl ring) is first order, implying that the oxidation of ebselen itself would also be first order.

Based on our calculations, the oxidation of the model ebselen compound proceeds via a two-step pathway (see Figure 8) in which the peroxide abstracts a proton from the amine generating a water molecule and the remaining OH of the peroxide bonds to the Se atom generating the first product complex (PC1). The second (fast) step involves a six-membered ring transition structure (TS2) in which two protons are transferred: one back to the amine group from the water molecule and one from the OH to the water molecule resulting in the desired products (PC2). This scheme represents the lowest energy pathway from reactants to products and indeed the only path that was located.

The results of our calculations on the ebselen model system are summarized in Figure 5 and Table 1. Figure 5 illustrates the relative energetics of the process. The relative energies of the reactant complex (RC1), first transition state (TS1), first product complex (PC1), second transition state (TS2), and second product complex (PC2) are plotted. The first and last points in the figure are the sum of the individual reactant energies and the sum of the individual product energies, respectively. Table 1 shows the bond length (r) and electron density at the bond critical point (ρ_{BCP}) for relevant bonding environments in each of the five extrema in Figure 5.

In the first transition state (TS1), we see that the bond between N2 and H3 is weakening as the value for ρ_{BCP} decreases to 0.248 au from the RC1 value of 0.335 au (typical for a N−H bond) and then to 0.030 au in the intermediate product complex (PC1). Also, it can be seen that the bond between the two peroxide oxygen atoms has been essentially broken at this stage (0.295 au in RC1 versus 0.053 au in TS1 with no bonding interaction at all in PC1). By the first product complex, H3 has essentially been transferred to O9 and O11 has become coordinated to the selenium atom. The second transition state (TS2) involves two H transfers. H12 is drawn from O11 to O9 and H3 shifts back to N3 from O9, resulting in the final product complex (PC2).

In comparison with the sulfur analogue, it is noticed that the selenium-containing ebselen model has a higher barrier to reaction (56.7 kcal/mol versus 53.6 kcal/mol). This was not expected because it is well known that selenium antioxidants perform considerably faster than their sulfur-containing coun-

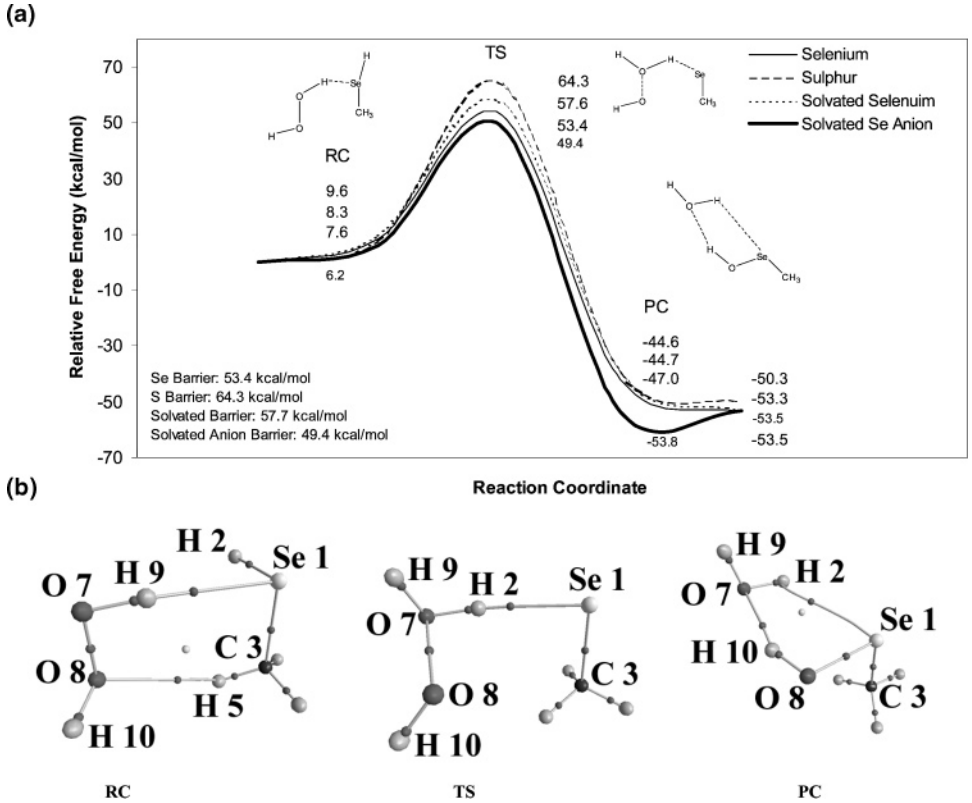

Figure 6. (a) Reaction energy profile for the model ebselen selenol reaction with hydrogen peroxide. Results are also presented for the sulfur analogue of the ebselen selenol model as well as the solvated selenium case. (b) Molecular graph of the reactant complex (RC), transition state (TS), and product complex (PC) showing positions of all nuclei, bond critical points (BCPs), and ring critical points (RCPs).

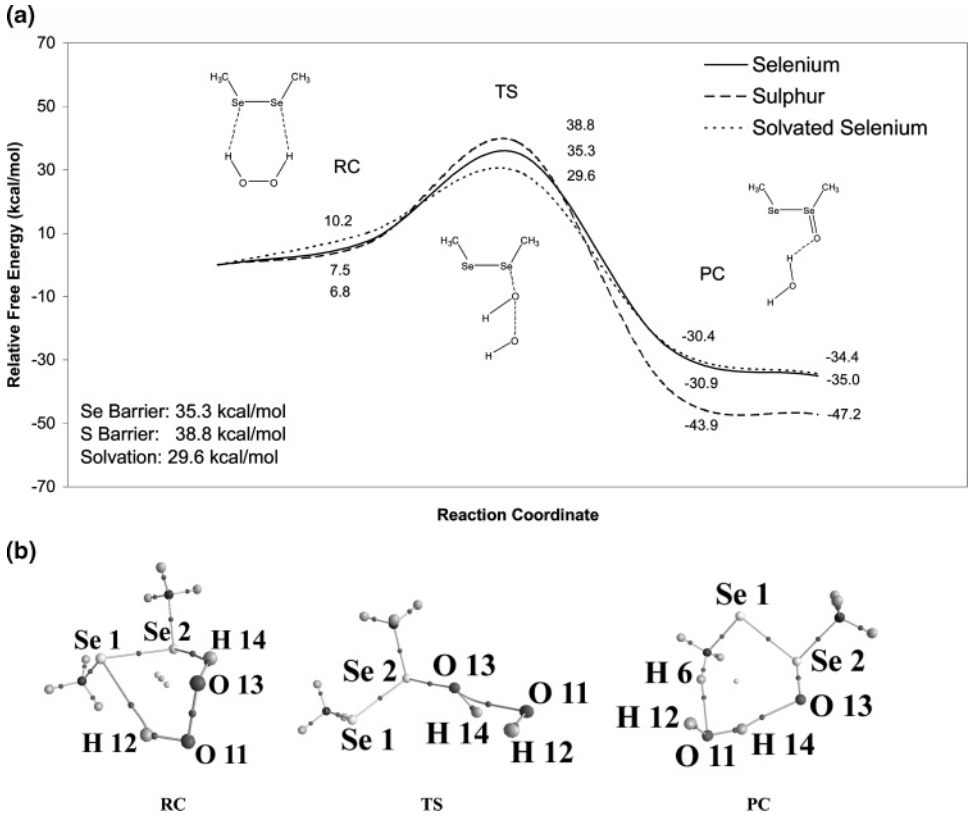

Figure 7. (a) Reaction energy profile for the model ebselen diselenide reaction with hydrogen peroxide. Results are also presented for the sulfur analogue of the ebselen diselenide model as well as the solvated selenium case. (b) Molecular graph of the reactant complex (RC), transition state (TS), and product complex (PC) showing positions of all nuclei, bond critical points (BCPs), ring critical points (RCPs), and the cage critical point (CCP).

terparts. However, it was also not expected that the amine hydrogen atom would participate in the process, and thus the apparent reversal in the trend is due to the proton transfer from the amine to the peroxide, which does not involve the sulfur or

TABLE 1: Interatomic Distances and Bond Critical Point Electron Densities of Relevant Interactions for the First Reactant Complex (RC1), First Transition State (TS1), First Product Complex (PC1), Second Transition State (TS2), and Second Product Complex (PC2) of the Ebselen Model Reaction

	RC1		TS1		PC1		TS2		PC2	
	r (Å)	ρ_{BCP} (au)	r (Å)	ρ_{BCP} (au)	r (Å)	ρ_{BCP} (au)	r (Å)	ρ_{BCP} (au)	r (Å)	ρ_{BCP} (au)
$Se_1–N_2$	1.839	0.169	1.784	0.191	1.713	0.219	1.766	0.201	1.837	0.176
$Se_1–C_5$	1.957	0.148	1.916	0.160	1.942	0.159	1.962	0.154	1.958	0.155
$Se_1–H_{10}$	2.465	0.021								
$Se_1–O_{11}$			2.710	0.027	1.811	0.166	1.711	0.205	1.645	0.234
$N_2–H_3$	1.015	0.335	1.115	0.248	1.974	0.030	1.318	0.142	1.025	0.325
$H_3–O_9$	2.427	0.010	1.420	0.099	0.982	0.340	1.181	0.188	2.077	0.021
$C_5–H_7$	1.089	0.280	1.106	0.269	1.089	0.278	1.089	0.276	1.090	0.279
$H_7–O_9$									2.488	0.008
$H_7–O_{11}$	1.583	0.007	1.954	0.029						
$O_9–H_{10}$	0.978	0.354	0.963	0.365	0.960	0.367	0.961	0.364	0.960	0.367
$O_9–O_{11}$	1.434	0.295	2.145	0.053						
$O_9–H_{12}$					1.872	0.031	1.282	0.142	0.983	0.338
$O_{11}–H_{12}$	0.965	0.371	0.964	0.355	0.983	0.338	1.155	0.200	1.801	0.037

TABLE 2: Interatomic Distances and Bond Critical Point Electron Densities of Relevant Interactions for the Reactant Complex (RC), Transition State (TS), and Product Complex (PC) of the Ebselen Selenol Model Reaction

	RC		TS		PC	
	r (Å)	ρ_{BCP} (au)	r (Å)	ρ_{BCP} (au)	r (Å)	ρ_{BCP} (au)
$Se_1–H_2$	1.469	0.177	2.118	0.043	2.726	0.013
$Se_1–C_3$	1.957	0.146	1.940	0.150	1.943	0.153
$Se_1–O_8$					1.795	0.167
$Se_1–H_9$	2.490	0.019				
$H_2–O_7$			1.013	0.306	0.967	0.358
$H_5–O_8$	2.595	0.008				
$O_7–H_9$	0.975	0.357	0.966	0.362	0.961	0.366
$O_7–O_8$	1.435	0.294	1.979	0.073		
$O_7–H_{10}$					1.896	0.030
$O_8–H_{10}$	0.964	0.372	0.971	0.361	0.976	0.349

TABLE 3: Interatomic Distances and Bond Critical Point Electron Densities of Relevant Interactions for the Reactant Complex (RC), Transition State (TS), and Product Complex (PC) of the Ebselen Diselenide Model Reaction

	RC		TS		PC	
	r (Å)	ρ_{BCP} (au)	r (Å)	ρ_{BCP} (au)	r (Å)	ρ_{BCP} (au)
$Se_1–Se_2$	2.326	0.107	2.333	0.107	2.403	0.098
$Se_1–H_{12}$	2.697	0.013				
$Se_2–H_{14}$	2.697	0.013				
$Se_2–O_{13}$			2.074	0.100	1.645	0.232
$H_6–O_{11}$					2.279	0.015
$O_{11}–H_{12}$	0.970	0.346	0.963	0.367	0.960	0.368
$O_{11}–O_{13}$	1.433	0.296	1.959	0.083		
$O_{11}–H_{14}$					0.974	0.349
$O_{13}–H_{14}$	0.970	0.364	0.990	0.324	1.866	0.030

selenium atom. Note that, in the second step of the reaction, the sulfur analogue does in fact have a higher free energy barrier, as expected. While the first sulfur product complex (PC1) is lower in energy than the corresponding selenium product complex, the sulfur-containing analogue shows a higher barrier for the second step relative to the selenium model compound.

Also, from Figure 5a it is apparent that the inclusion of the effects of solvation does not play a stabilizing role in the energetics of the reaction, as the barriers differ by 3.5 kcal/mol. While these are single-point solvation effects calculated using gas-phase structures, it is not expected that this condition should affect the results significantly as there is extensive precedent for incorporating solvation effects in this way.

Of course, the model ebselen compound used here has some serious limitations, especially in light of the participation of the amine hydrogen atom. Ebselen itself does not have any available protons on the nitrogen adjacent to the selenium atom, and so this mechanism is not feasible for the real system. The effect of this limitation will be the focus of a future paper.

Ebselen Selenol Oxidation. The selenol form of ebselen is the one that most closely resembles that of the active site Sec residue in GPx and other selenoproteins, and despite several proposed mechanisms it is suspected that this molecule represents the key antioxidant form in the GPx cycle of ebselen.[63] Indeed, the path **2** → **6** → **7** is quite similar to the GPx reductive pathway (see Figure 1).

The results of our calculations on the ebselen selenol model are summarized in Figure 6 and Table 2. It is an exothermic one-step process that first involves a proton abstraction from the Se or S atom by the peroxide. By examining bond lengths and ρ_{BCP} (Table 2) for relevant bonds in the reactant complex, the transition state, and the product complex, a clear interpretation of the reaction mechanism can be made. At the transition state, H2 is almost completely transferred to O7 from Se1, creating a water molecule. The bond between O7 and O8 is also broken, leaving a lone OH group that will then bond to Se1 giving the desired products. The barrier to this reaction is 53.4 kcal/mol for Se and 64.3 kcal/mol for S. The higher barrier for the sulfur analogue reflects the experimentally observed trend of sulfur being a less efficient antioxidant. As with the case of the ebselen model, the effects of solvation are not large and result in destabilization of the transition state.

While the barrier is lower for the ebselen selenol case than the ebselen case, supporting the idea of the ebselen selenol molecule being a more viable antioxidant, the absolute values do not suggest a fast reaction, as experiment would dictate. Even when the effects of solvation are included, the barriers do not become more realistic for a catalytic process; in fact, they become larger. This is the motivation for including the deprotonated anion of the ebselen selenol model in this study. The anion results are also included in Figure 6a. The barrier is similar to that of the neutral selenol case; however, there is a decrease of approximately 4 kcal/mol. There is added stability associated with the reactant complex due to strong electrostatic attraction. This attraction is also sufficient to distort the approaching

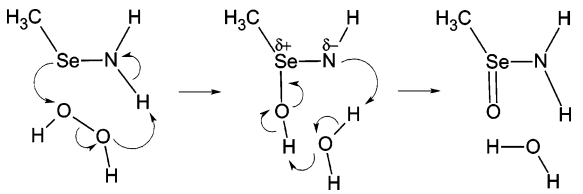

Figure 8. A proposed mechanism for the reaction of the model ebselen compound with hydrogen peroxide.

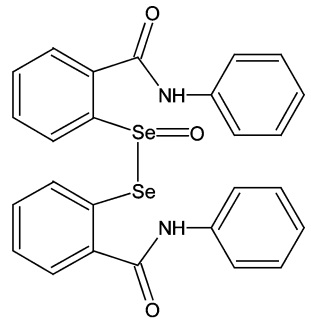

15

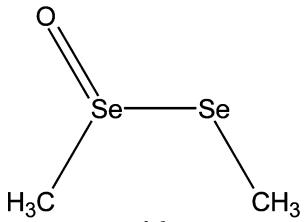

16

Figure 9. Proposed products of the ebselen diselenide reaction (**15**) and ebselen diselenide model reaction (**16**) with hydrogen peroxide.

hydrogen peroxide dihedral to approximately 20°. In the transition state, a proton is transferred from one oxygen atom to the other as the resulting selenium oxide bond is formed.

Ebselen Diselenide Oxidation. Experimental investigation of the oxidation of diselenides has led to the proposed product in Figure 3 (**8**), which is actually thought to be a short-lived intermediate along the path to either the original ebselen molecules or the more highly oxidized seleninic acids.[47−49,64] In contrast, our results indicate that the product of such an oxidation may in fact be a diselenide with an oxygen atom bonded to only one of the two selenium atoms rather than being inserted between them. All attempts to locate a reaction path between the ebselen diselenide model and the corresponding oxidation product in Figure 4 (**14**) have led to the product in Figure 9 (**16**). It is interesting to note that Kice and Chiou first postulated that the oxidation of a diselenide would result in an oxygen atom being inserted between the selenium atoms (**8**) only after a fast isomerization of the product in Figure 9 (**15**).[64] However, calculations on our model system show that isomer **16** is actually lower in energy than **14** by 12 kcal/mol, suggesting that **14** may not be formed at all (at least not by a fast isomerization of **16**), which calls the existence of **8** into question in the context of these reactions. In addition, no experimental evidence for the existence of **8** has been reported to date, which could also be due to the short lifetimes of these reactive intermediates.

The results of our calculations on the ebselen diselenide model compound are summarized in Figure 7 and Table 3. The reaction is exothermic with a barrier of 35.3 kcal/mol for Se and 38.8 kcal/mol for S, again reflecting the stronger antioxidant behavior of selenium. In this case, solvation does play a significant role and results in a stabilization of the transition state of about 6 kcal/mol, bringing the overall solvated reaction barrier to 29.6 kcal/mol.

The primary development in proceeding from the reactant complex (RC) to transition state (TS) in this reaction is the breaking of the O11−O13 bond (seen in Table 3 by ρ_{BCP} decreasing from 0.296 au, typical of an oxygen−oxygen single bond, to 0.083 au). Also, in the transition state, O13 develops a bonding interaction to Se2. H14 is finally transferred to O11, and the products are formed.

On the basis of our data, the diselenide oxidation is predicted to be the fastest due to a relatively low barrier to reaction. This agrees with the experiment of Fischer and Dereu,[47] who qualitatively determined that the reaction of ebselen diselenide with hydrogen peroxide must be much faster than that of ebselen with hydrogen peroxide.

TABLE 4: Summary of Free Energy Barriers and Reaction Enthalpies (in kcal/mol) for All Processes Studied in This Paper

reaction	free energy barrier (kcal/mol)	reaction enthalpy (kcal/mol)
ebselen model oxidation (step 1)	56.7	−37.7
ebselen model oxidation (step 2)	6.4	−9.1
solvated ebselen model oxidation (step 1)	60.2	−37.5
solvated ebselen model oxidation (step 2)	8.5	−10.4
ebselen model oxidation with S (step 1)	53.6	−46.9
ebselen model oxidation with S (step 2)	8.1	−12.7
ebselen selenol model oxidation	53.4	−56.3
solvated ebselen selenol model oxidation	57.7	−54.0
ebselen selenol model oxidation with S	64.3	−53.9
ebselen selenol model anion oxidation	49.4	−56.5
ebselen diselenide model oxidation	35.3	−39.5
solvated ebselen diselenide model oxidation	29.6	−40.2
ebselen selenol model oxidation with S	38.8	−52.3

Conclusions

Density functional theory calculations on a series of model reactions designed to elucidate the reactivity and energetics of selenium-containing antioxidants, particularly ebselen, have been performed. The reactions studied were oxidations of an ebselen model, an ebselen selenol model, and an ebselen diselenide model by hydrogen peroxide. The calculations have been repeated for the sulfur analogues of these model systems, and the effects of solvation have been included. In the case of the ebselen selenol model, the explicitly solvated anion was also considered.

Reaction energy barriers for the ebselen, ebselen selenol, and ebselen diselenide models are 56.7, 53.4, and 35.3 kcal/mol, respectively. Other barriers and reaction enthalpies are summarized in Table 4. The relatively high barriers of these reactions (as compared to what might be expected of a catalytic process) may be due, in part, to the fact that they are small molecule models of the enzyme mimics. Unfortunately, to the best of our knowledge, there is no available experimental kinetic data for comparison. Effects of solvation are generally small but account for a significant lowering of the diselenide model barrier (29.6 kcal/mol), making it the clearly favored reaction of all tested, which agrees with the available experimental findings. A comparison to the sulfur analogues of all molecules studied shows that, in general, sulfur increases the reaction barrier, in agreement with experimental results.

Our data show that of the three plausible oxidation pathways for ebselen and its derivatives, that of the diselenide is favored. This result is supported by recent evidence of highly efficient GPx mimics in the literature based on a diselenide framework.[65]

Acknowledgment. We gratefully acknowledge the Natural Sciences and Engineering Research Council of Canada (NSERC) and the Killam Trusts for financial support. We also would like to acknowledge Leif Eriksson for thoughtful discussion as well as computational resources.

Supporting Information Available: Archive entries for calculations involved in Figures 5−7 (Tables S1−S3, respectively). This material is available free of charge via the Internet at http://pubs.acs.org.

References and Notes

(1) Flohé, L.; Loschen, G.; Günzler, W. A.; Eichele, E. *Hoppe-Seyler's Z. Physiol. Chem.* **1972**, *353*, 987.

(2) *Selenium in Biology and Human Health*; Burk, R. F., Ed.; Springer-Verlag: New York, 1994.

(3) Flohé, L. *Curr. Top. Cell. Regul.* **1985**, *27*, 473.

(4) Tappel, A. L. *Curr. Top. Cell. Regul.* **1984**, *24*, 87.

(5) Epp, O.; Ladenstein, R.; Wendel, A. *Eur. J. Biochem.* **1983**, *133*, 51.

(6) *Free Radicals in Biology*; Pryor, W. A., Ed.; Academic Press: New York, 1976−1982; Vols. 1−5.

(7) *Free Radicals in Molecular Biology, Aging and Disease*; Armstrong, D., Sohal, R. S., Cutler, R. G., Slater, T. F., Eds.; Raven Press: New York, 1984.

(8) Ganther, H. E. *Chem. Scr.* **1975**, *8a*, 79.

(9) Ganther, H. E.; Kraus, R. J. In *Methods in Enzymology*; Colowick, S. P., Kaplan, N. O., Eds.; Academic Press: New York, 1984; Vol. 107, pp 593−602.

(10) Stadtman, T. C. *J. Biol. Chem.* **1991**, *266*, 16257.

(11) Aumann, K. D.; Bedorf, N.; Brigelius-Flohé, R.; Schomburg, D.; Flohé, L. *BES* **1997**, *10*, 136.

(12) Flohé, L. In *Glutathione: Chemical, Biochemical and Medical Aspects*; Dolphin, D., Poulson, R., Avramovic, O., Eds.; John Wiley & Sons: New York, 1989; pp 643−731.

(13) Benkova, Z.; Kóňa, J.; Gann, G.; Fabian, W. M. F. *Int. J. Quantum Chem.* **2002**, *90*, 555.

(14) Mugesh, G.; Panda, A.; Singh, H. B.; Punekar, N. S.; Butcher, R. J. *J. Am. Chem. Soc.* **2001**, *123*, 839.

(15) Bailly, F.; Azaroual, N.; Bernier, J. L. *Bioorg. Med. Chem.* **2003**, *11*, 4623.

(16) Back, T. G.; Moussa, Z. *J. Am. Chem. Soc.* **2003**, *125*, 13455−13460.

(17) Mugesh, G.; Du Mont, W. W. *Chem.-Eur. J.* **2001**, *7*, 1365.

(18) Mugesh, G.; Singh, H. B. *Chem. Soc. Rev.* **2000**, *29*, 347.

(19) Wirth, T. *Molecules* **1998**, *3*, 164.

(20) Wilson, S. R.; Zucker, P. A.; Huang, R.-R. C.; Spector, A. *J. Am. Chem. Soc.* **1989**, *111*, 5936.

(21) Reich, H. J.; Jasperse, C. P. *J. Am. Chem. Soc.* **1987**, *109*, 5549.

(22) Iwaoka, M.; Tomoda, S. *J. Am. Chem. Soc.* **1996**, *118*, 8077.

(23) Mugesh, G.; Panda, A.; Singh, H. B.; Punekar, N. S.; Butcher, R. J. *J. Chem. Soc., Chem. Commun.* **1998**, 2227.

(24) Galet, V.; Bernier, J. L.; Heniehart, J. P.; Lesieur, D.; Abadie, C.; Rochette, L.; Lindenbaum, A.; Chalas, J.; Renaud de la Faverie, J. F.; Pfeiffer, B.; Renard, P. *J. Med. Chem.* **1994**, *37*, 2903.

(25) Iwaoka, M.; Tomoda, S. *J. Am. Chem. Soc.* **1994**, *116*, 2557.

(26) Müller, A.; Cadenas, E.; Graf, P.; Sies, H. *Biochem. Pharmacol.* **1984**, *33*, 3235.

(27) Wendel, A.; Fausel, M.; Safayhi, H.; Tiegs, G.; Otter, R. *Biochem. Pharmacol.* **1984**, *33*, 3241.

(28) Parnham, M. J.; Kindt, S. *Biochem. Pharmacol.* **1984**, *33*, 3247.

(29) Müller, A.; Gabriel, H.; Sies, H. *Biochem. Pharmacol.* **1985**, *34*, 1185.

(30) Safayhi, H.; Tiegs, G.; Wendel, A. *Biochem. Pharmacol.* **1985**, *34*, 2691.

(31) Wendel, A.; Tiegs, G. *Biochem. Pharmacol.* **1986**, *35*, 2115.

(32) Zhao, R.; Masayasu, H.; Holmgren, A. *Proc. Natl. Acad. Sci. U.S.A.* **2002**, *99*, 8579.

(33) Wendel, A.; Fausel, M.; Safayhi, H.; Tiegs, G.; Otter, R. *Biochem. Pharmacol.* **1984**, *33*, 3241.

(34) Müller, A.; Cadenas, E.; Graf, P.; Sies, H. *Biochem. Pharmacol.* **1984**, *33*, 3235.

(35) Parnham, M. J.; Kindt, S. *Biochem. Pharmacol.* **1984**, *33*, 3247.

(36) Fong, M. C.; Schiesser, C. H. *Tetrahedron Lett.* **1995**, *36*, 7329.

(37) Sies, H. *Free Radical Biol. Med.* **1993**, *14*, 313.

(38) Sies, H. *Methods Enzymol.* **1994**, *234*, 476.

(39) Schewe, T. *Gen. Pharmacol.* **1995**, *26*, 1153.

(40) Nakamura, Y.; Feng, Q.; Kumagi, T.; Torikai, K.; Ohigashi, H.; Osawa, T.; Noguchi, N.; Niki, E.; Uchida, K. *J. Biol. Chem.* **2002**, *277*, 2687.

(41) Zhang, M.; Nomura, A.; Uchida, Y.; Iijima, H.; Sakamoto, T.; Iishii, Y.; Morishima, Y.; Mochizuki, M.; Masuyama, K.; Hirano, K.; Sekizawa, K. *Free Radical Biol.* **2002**, *32*, 454.

(42) Fischer, H.; Terlinden, R.; Lohr, J. P.; Romer, A. *Xenobiotica* **1988**, *18*, 1347.

(43) Müller, A.; Gabriel, H.; Sies, H.; Terlinden, R.; Fischer, H.; Romer, A. *Biochem. Pharmacol.* **1988**, *37*, 1103.

(44) Sies, H. In *Selenium in Biology and Medicine*; Wendel, A., Ed.; Springer-Verlag: Heidelberg, 1989; pp 153−162.

(45) Zhao, R.; Holmgren, A. *J. Biol. Chem.* **2002**, *277*, 39456.

(46) Engman, L.; Stern, D.; Cotgreave, I. A.; Andersson, C. M. *J. Am. Chem. Soc.* **1992**, *114*, 9737.

(47) Fischer, H.; Dereu, N. *Bull. Soc. Chim. Belg.* **1987**, *96*, 757.

(48) Haenen, G. R. M. M.; De Rooij, B. M.; Vermeulen, N. P. E.; Bast, E. *Mol. Pharmacol.* **1990**, *37*, 412.

(49) Glass, R. S.; Farooqui, F.; Sabahi, M.; Ehler, K. W. *J. Org. Chem.* **1989**, *54*, 1092.

(50) Back, T. G.; Moussa, Z. *J. Am. Chem. Soc.* **2003**, *125*, 13455.

(51) Pearson, J. K.; Ban, F.; Boyd, R. J. *J. Phys. Chem.* **2005**, *109*, 10373.

(52) Frisch, M. J.; Trucks, G. W.; Schlegel, H. B.; Scuseria, G. E.; Robb, M. A.; Cheeseman, J. R.; Montgomery, J. A., Jr.; Vreven, T.; Kudin, K. N.; Burant, J. C.; Millam, J. M.; Iyengar, S. S.; Tomasi, J.; Barone, V.; Mennucci, B.; Cossi, M.; Scalmani, G.; Rega, N.; Petersson, G. A.; Nakatsuji, H.; Hada, M.; Ehara, M.; Toyota, K.; Fukuda, R.; Hasegawa, J.; Ishida, M.; Nakajima, T.; Honda, Y.; Kitao, O.; Nakai, H.; Klene, M.; Li, X.; Knox, J. E.; Hratchian, H. P.; Cross, J. B.; Adamo, C.; Jaramillo, J.; Gomperts, R.; Stratmann, R. E.; Yazyev, O.; Austin, A. J.; Cammi, R.; Pomelli, C.; Ochterski, J. W.; Ayala, P. Y.; Morokuma, K.; Voth, G. A.; Salvador, P.; Dannenberg, J. J.; Zakrzewski, V. G.; Dapprich, S.; Daniels, A. D.; Strain, M. C.; Farkas, O.; Malick, D. K.; Rabuck, A. D.; Raghavachari, K.; Foresman, J. B.; Ortiz, J. V.; Cui, Q.; Baboul, A. G.; Clifford, S.; Cioslowski, J.; Stefanov, B. B.; Liu, G.; Liashenko, A.; Piskorz, P.; Komaromi, I.; Martin, R. L.; Fox, D. J.; Keith, T.; Al-Laham, M. A.; Peng, C. Y.; Nanayakkara, A.; Challacombe, M.; Gill, P. M. W.; Johnson, B.; Chen, W.; Wong, M. W.; Gonzalez, C.; Pople, J. A. *Gaussian 03*, revision B.05; Gaussian, Inc.: Pittsburgh, PA, 2003.

(53) Becke, A. D. *J. Chem. Phys.* **1993**, *98*, 5648.

(54) Perdew, J. P.; Wang, Y. *Phys. Rev. B* **1992**, *45*, 13244.

(55) Peng, C.; Schlegel, H. B. *Isr. J. Chem.* **1993**, *33*, 449.

(56) Peng, C.; Ayala, P. Y.; Schlegel, H. B.; Frisch, M. J. *J. Comput. Chem.* **1996**, *17*, 49.

(57) Gonzalez, C.; Schlegel, H. B. *J. Chem. Phys.* **1989**, *90*, 2154.

(58) Gonzalez, C.; Schlegel, H. B. *J. Phys. Chem.* **1990**, *94*, 5523.

(59) Biegler-König, F. W.; Schönbohm, J.; Bayles, D. *J. Comput. Chem.* **2001**, *22*, 545.

(60) Biegler-König, F. W.; Schönbohm, J.; Bayles, D. The AIM2000 program can be downloaded from the Internet at http://gauss.fh-bielefeld.de/aim2000.

(61) Bader, R. F. W. *Atoms in Molecules: A Quantum Theory*; Oxford University Press: Oxford, U.K., 1990.

(62) Castillo, N.; Matta, C. F.; Boyd, R. J. *Chem. Phys. Lett.* **2005**, *409*, 265.

(63) Sarma, B. K.; Mugesh, G. *J. Am. Chem. Soc.* **2005**, *127*, 11477.

(64) Kice, J. L.; Chiou, S. *J. Org. Chem.* **1986**, *51*, 290.

(65) Zhang, X.; Xu, H.; Dong, Z.; Wang, Y.; Liu, J.; Shen, J. *J. Am. Chem. Soc.* **2004**, *126*, 10556.